Wireless Personal Communications **23:** 31–44, 2002.

Performance of Multi-Antenna Signaling Strategies Using Dual-Polarized Antennas: Measurement Results and Analysis

ROHIT U. NABAR [3], VINKO ERCEG [2], HELMUT BÖLCSKEI [3] and AROGYASWAMI J. PAULRAJ [1]

[1] *Information Systems Laboratory, Stanford University, 272 David Packard Building, 350 Serra Mall, Stanford, CA 94305, U.S.A.*
E-mail: apaulraj@stanford.edu
[2] *Zyray Wireless, 11455 El Camino Real, Suite 350, San Diego, CA 92130, U.S.A.*
E-mail: verceg@ZYRAYwireless.com
[3] *Communication Technology Laboratory, Swiss Federal Institute of Technology (ETH) Zürich ETH Zentrum, ETF E122, Sternwartstrasse 7, CH-8092 Zürich, Switzerland*
E-mail: {nabar,boelcskei}@nari.ee.ethz.ch

Abstract. Multiple-input multiple-output (MIMO) wireless systems employ spatial multiplexing to increase spectral efficiency or transmit diversity (space-time coding) techniques to improve link reliability. The performance of these signaling techniques is highly dependent on channel characteristics which in turn depend on antenna height and spacing and richness of scattering. The use of dual-polarized antennas is a cost- and space-effective alternative where two spatially separated uni-polarized antennas can be replaced by a single dual-polarized antenna element. In this paper, we use fixed-wireless experimental data collected in a typical suburban environment at 2.5 GHz to investigate the performance of spatial multiplexing and transmit diversity (Alamouti scheme) for a dual-polarized antenna setup. Channel measurements were conducted over a cell of radius 7 km and channel statistics such as K-factor, cross-polarization discrimination (XPD), and fading signal correlation were extracted from the gathered data. At each location, different combinations of these parameters yield different performance (measured in terms of average uncoded bit error rate) of spatial multiplexing and the Alamouti scheme. The results indicate that proper selection of the transmission mode through feedback, if possible, can reduce the bit error rate by several orders of magnitude. Furthermore, the results hint at the existence of a preferred-mode switching distance within a cell – above/below which one mode of transmission exhibits generally superior performance.

Keywords: MIMO wireless, channel measurements, polarization diversity, spatial multiplexing, Alamouti scheme, preferred-mode switching distance.

1. Introduction

The use of multiple antennas at both ends of a wireless link (MIMO technology) has recently been shown to have the potential of drastically increasing spectral efficiency through a technique known as *spatial multiplexing* [1–5]. This leverage often referred to as *multiplexing gain* permits the opening of multiple spatial data pipes between transmitter and receiver within the frequency band of operation for no additional power expenditure, leading to a linear increase in capacity. Multiple antennas at both ends of a wireless link can also be used to improve link reliability through the use of *transmit diversity* techniques such as space-time coding [6–9], a leverage that is referred to as *diversity gain*. Diversity gain reduces the receive signal level fluctuation and improves the quality of transmission. Multiplexing and diversity gain in MIMO systems depend strongly on the channel characteristics which in turn depend on

transmit and receive antenna height and spacing and the scattering environment. In practice, antenna spacings of several tens of wavelengths at the base-station and up to a wavelength at the subscriber unit are required in order to achieve significant multiplexing or diversity gain. Space to support multiple antennas is generally expensive or even unavailable, more so at the subscriber unit than at the base-station. The use of polarization diversity, particularly dual-polarized antennas, is a promising cost- and space-effective alternative where two spatially separated uni-polarized antennas can be replaced by a single antenna structure employing orthogonally polarized elements.

In practice, propagation conditions often clearly favor one of the two above mentioned signaling modes (spatial multiplexing and transmit diversity). It is therefore paramount to understand and identify channel conditions that suit one mode over the other [10].

Contributions. In this paper, we investigate the performance of uncoded spatial multiplexing and transmit diversity, in particular the *Alamouti scheme* [9] using data acquired from channel measurements. The data extracted from the measurements includes Ricean K-factor, cross-polarization discrimination (XPD) and fading signal correlation coefficients. We use previously developed techniques [10, 11] to evaluate the performance of spatial multiplexing and the Alamouti scheme over a cell of radius 7 km for a fixed data rate and signal-to-noise ratio (SNR) at each location. Performance is measured in terms of average uncoded bit error rate (BER). The results indicate that making minimal feedback regarding the channel statistics available to the transmitter combined with appropriate selection of the transmission mode can result in several orders of magnitude improvement in BER. Selecting the optimal transmission mode based on instantaneous channel knowledge at the transmitter has been studied in [12]. Conveying channel statistics to the transmitter can be accomplished via a low-bandwidth feedback link and is much easier to realize than feeding back the channel state information itself. Additionally, our results point to the existence of a preferred-mode switching distance within a cell – above/below which one mode of transmission exhibits generally superior performance.

Organization of the paper. The rest of this paper is organized as follows. Section 2 describes the measurement system used and the setup for the measurement campaign. Section 3 reviews the channel model validated by the measurements. Section 4 briefly describes the performance analysis techniques. We present our results in Section 5, and conclude in Section 6.

2. Measurement System and Setup

2.1. Measurement System

A custom measurement system [13] was designed and implemented in hardware, which allowed the measurement of a MIMO channel at 2.48 GHz center frequency. The system was based on swept frequency sounding with a narrow-band test signal swept in 200 kHz steps across a 4 MHz frequency band every 84 ms. The narrow-band receiver was swept synchronously with the transmitter, with timing references derived from rubidium clocks. The advantage of this design is a low noise floor (narrow bandwidth) and reduced complexity compared to spread spectrum measurement systems. Figure 1 shows the configuration of the measurement system. Control and measurement signals were created using programmable RF signal generators. The recorded channel response data was streamed to computer hard disc for later processing using C++ and Matlab.

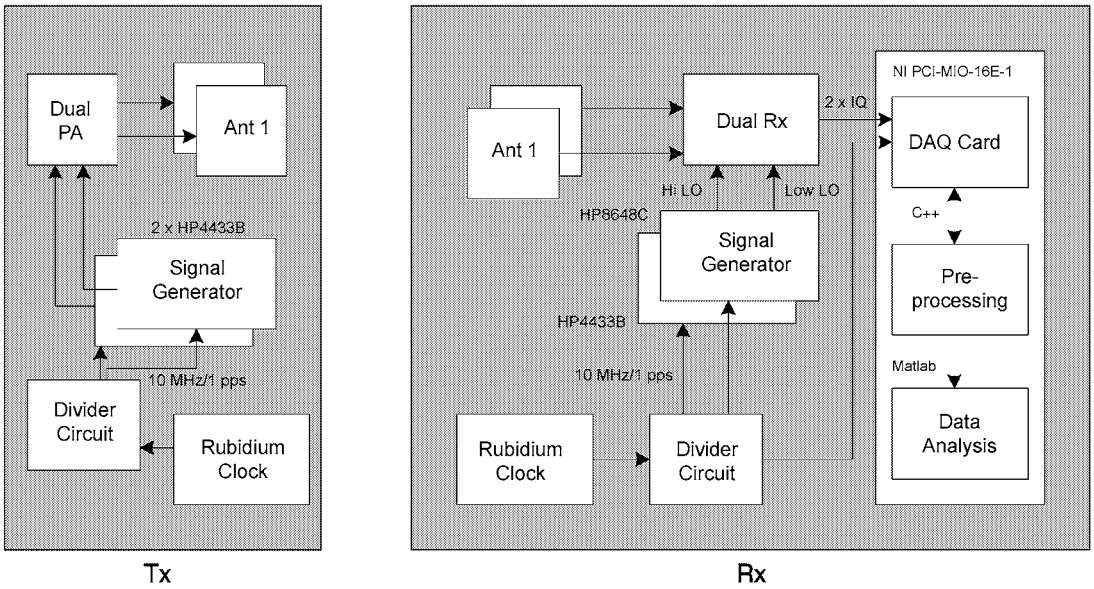

Figure 1. Schematic of measurement system.

2.2. Measurement Setup

In the measurements, a dual-polarized receive antenna with slanted polarizations (co-located $\pm 45°$), a gain of 12 dBi and an azimuthal beam-width of 90° was used. The antenna was mounted on a retractable mast of height 3 m. The +45° and –45° polarization transmit antennas separated by 10 wavelengths were also directive with an azimuthal beam-width of 90° and a gain of 17 dBi. Figure 2 depicts the antenna configuration for the measurement campaign. The transmitter was located on top of an office building with an antenna height of nearly 20 m above the street level. Outdoor measurements at 58 fixed locations with the receiver located at the curbside were conducted in the San Francisco Bay Area over a cell of radius 7 km. At each location, two measurements 1 m apart were taken. Therefore, the total number of measurements was 116. Each measurement was taken over a 5 minute interval in the direction of the strongest signal which turned out to be the direct transmitter-receiver path in most cases. The terrain can be characterized as mostly suburban and flat with moderate tree and building density. The average building and tree height was about 15 m. When conducting the measurements, the received SNR was greater than 25 dB, even at the cell edge, ensuring high reliability of the channel statistics extracted from the measurement data.

3. Channel Model

In this section, we briefly discuss the narrow-band channel model [10, 11] that is validated by the measurements for the setup under consideration. The input-output relation for the channel model is given by

$$\boldsymbol{r} = \boldsymbol{H}\,\boldsymbol{x} + \boldsymbol{n}, \tag{1}$$

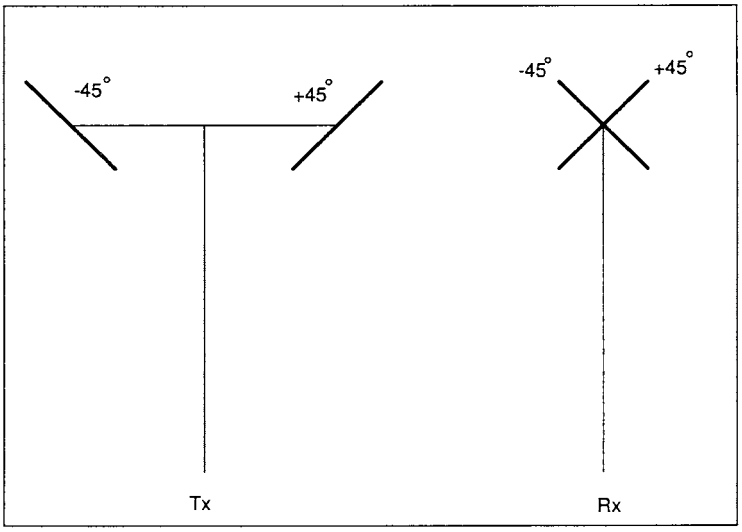

Figure 2. Schematic of antenna configuration.

where[1]

- $\boldsymbol{x} = [x_0 \;\; x_1]^T$ is the 2×1 transmit signal vector whose elements are taken from a finite (complex) constellation,
- $\boldsymbol{r} = [r_0 \;\; r_1]^T$ is the 2×1 receive signal vector,
- $\boldsymbol{n}$ is the 2×1 temporally i.i.d. zero-mean complex Gaussian noise vector with $\mathcal{E}\{\boldsymbol{n}\boldsymbol{n}^H\} = \sigma_n^2 \boldsymbol{I}_2$,
- $\boldsymbol{H} = \begin{bmatrix} h_{0,0} & h_{0,1} \\ h_{1,0} & h_{1,1} \end{bmatrix}$ is the channel transfer or polarization matrix.

The polarization matrix $\boldsymbol{H}$ describes the degree of suppression of individual co-and cross-polarized components, cross-correlation, and cross-coupling of energy from one polarization state to the other polarization state. The signals x_0 and x_1 are transmitted on the two different polarizations, and r_0 and r_1 are the signals received on the corresponding polarizations. We emphasize that the underlying channel is a 2-input 2-output channel, since each polarization mode is treated as a separate physical channel. The elements of $\boldsymbol{H}$ are (in general correlated) complex Gaussian random variables. Without loss of generality, the channel matrix may be expressed as the sum of a fixed (possibly line-of-sight) component and a scattered (or variable) component as follows

$$\boldsymbol{H} = \sqrt{\frac{K}{1+K}}\,\overline{\boldsymbol{H}} + \sqrt{\frac{1}{1+K}}\,\widetilde{\boldsymbol{H}}, \tag{2}$$

where $\mathcal{E}\{\mathbf{H}\} = \sqrt{\frac{K}{1+K}}\,\overline{\boldsymbol{H}}$ and $\sqrt{\frac{1}{1+K}}\,\widetilde{\boldsymbol{H}}$ are the average and variable component of the channel matrix, respectively. The factors $\sqrt{\frac{K}{1+K}}$ and $\sqrt{\frac{1}{1+K}}$ in (2) are energy normalization factors and are related to the K-factor as will be described later. The elements of the matrix $\widetilde{\boldsymbol{H}}$, denoted as

[1] The superscripts ^{T} and ^{H} stand for transpose and conjugate transpose, respectively. $\mathcal{E}$ is the expectation operator and $\boldsymbol{I}_m$ is the identity matrix of dimension $m \times m$.

$\widetilde{h}_{i,j}$ $(i, j = 0, 1)$, are zero-mean complex Gaussian random variables whose variances depend on the propagation conditions. Throughout this paper, we assume

$$\mathcal{E}\{|\widetilde{h}_{0,0}|^2\} = \mathcal{E}\{|\widetilde{h}_{1,1}|^2\} = 1 \tag{3}$$

$$\mathcal{E}\{|\widetilde{h}_{0,1}|^2\} = \mathcal{E}\{|\widetilde{h}_{1,0}|^2\} = \alpha\,, \tag{4}$$

where $0 < \alpha \leq 1$ is directly related to the XPD (or separation of orthogonal polarizations) for the variable component of the channel. Good discrimination of orthogonal polarizations amounts to small values of α and vice versa. We note that α is not only a function of the antenna elements' ability to separate orthogonal polarizations but also of the propagation environment (coupling between orthogonal polarizations due to scattering). The elements of the matrix $\overline{\boldsymbol{H}}$, denoted as $\overline{h}_{i,j}$ $(i, j = 0, 1)$, satisfy

$$|\overline{h}_{0,0}|^2 \;=\; |\overline{h}_{1,1}|^2 \;= 1 \tag{5}$$

$$|\overline{h}_{0,1}|^2 \;=\; |\overline{h}_{1,0}|^2 \;= \alpha_f\,, \tag{6}$$

where $0 \leq \alpha_f \leq 1$ is directly related to the XPD for the fixed component of the channel. It is important to note that the presence of a fixed channel component does not always imply line-of-sight transmission. For pure line-of-sight conditions (for example, very high transmit and receive antennas) α_f unlike α is solely a function of the antennas' ability to separate the orthogonal polarizations.

The Ricean K-factor of a fading channel is defined as the ratio of the power in the fixed component to the power in the scattered component [14]. Under the assumptions made above, the K-factor for each element of the channel matrix, $K_{i,j}$ $(i, j = 0, 1)$, can be expressed as follows

$$K_{0,0} \;=\; K_{1,1} \;=\; K \tag{7}$$

$$K_{0,1} \;=\; K_{1,0} \;=\; \frac{\alpha_f}{\alpha} K\,. \tag{8}$$

For the remainder of this paper, we shall refer to K as the K-factor of the system. Experimental data reveals that the elements of $\boldsymbol{H}$ are in general correlated. We define the following correlation coefficients[2]

$$t = \frac{\mathcal{E}\{\widetilde{h}_{0,0}\widetilde{h}^*_{0,1}\}}{\sqrt{\alpha}} = \frac{\mathcal{E}\{\widetilde{h}_{1,0}\widetilde{h}^*_{1,1}\}}{\sqrt{\alpha}} \tag{9}$$

$$r = \frac{\mathcal{E}\{\widetilde{h}_{0,0}\widetilde{h}^*_{1,0}\}}{\sqrt{\alpha}} = \frac{\mathcal{E}\{\widetilde{h}_{0,1}\widetilde{h}^*_{1,1}\}}{\sqrt{\alpha}} \tag{10}$$

$$s = \mathcal{E}\{\widetilde{h}_{0,0}\widetilde{h}^*_{1,1}\} \approx \frac{\mathcal{E}\{\widetilde{h}_{0,1}\widetilde{h}^*_{1,0}\}}{\alpha}\,, \tag{11}$$

where t is referred to as the transmit correlation coefficient while r is referred to as the receive correlation coefficient. The correlation coefficient s captures the correlation of the diagonal

[2] The superscript * stands for complex conjugate.

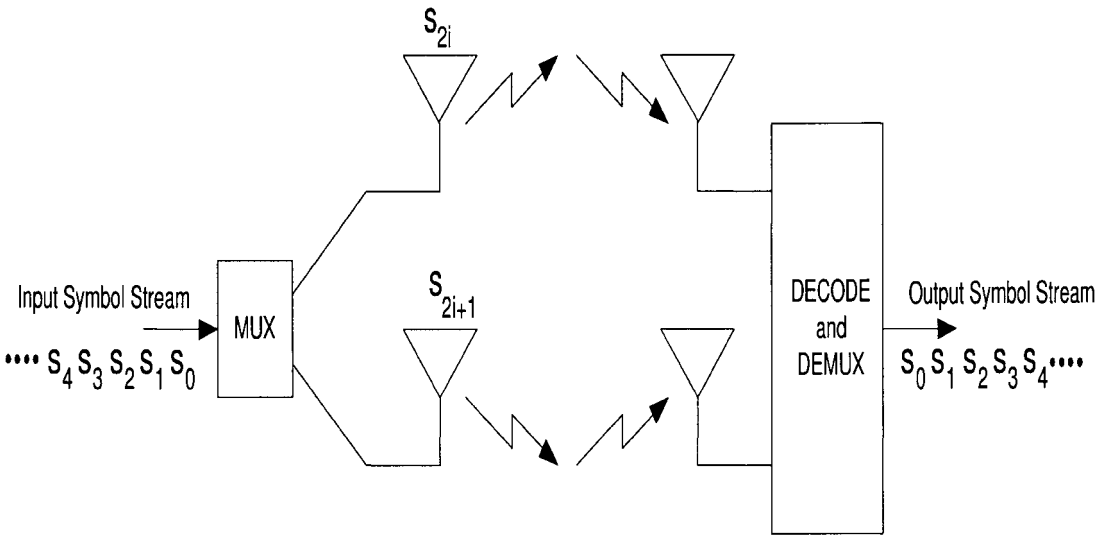

Figure 3. Spatial multiplexing.

and the anti-diagonal elements, respectively. The approximation sign in (11) is motivated by measurement results. The experimental data gathered during the measurement campaign was used to extract values of K, α_f, α, r, t, and s for each measurement location. Using these statistical parameters, it is possible to estimate the performance of spatial multiplexing and the Alamouti scheme in terms of average uncoded symbol error rate as will be described in the next section. It is pertinent to note that in addition to the channel statistics mentioned above, knowledge of the fixed component of the channel matrix, $\overline{\boldsymbol{H}}$, is required to estimate the symbol error rate. Due to limitations in the measurement equipment, determination of the phase information of $\overline{\boldsymbol{H}}$ was not possible. Instead, we resorted to random computer generated realizations of $\overline{\boldsymbol{H}}$.

4. Performance Analysis

4.1. Spatial Multiplexing

MIMO systems employ spatial multiplexing to increase spectral efficiency. Figure 3 shows a schematic of a spatial multiplexing system. The symbol stream to be transmitted is split up into two sub-streams each of which is launched from one of the two orthogonal polarizations. We assume that the receiver has perfect channel knowledge (acquired through training) and performs maximum-likelihood (ML) detection. In the following, we shall use an estimate $\bar{P}_{mux}$ of the average (over the random channel) uncoded scalar symbol error rate for spatial multiplexing as a function of the channel statistics derived in [10, 11]. The estimate relies on a weighted average pairwise error probability (PEP) approach and provides an estimate of the symbol error rate that matches the actual symbol error rate very closely. Furthermore, $\bar{P}_{mux}$ reveals all the trends of the actual symbol error rate with varying channel statistics and SNR, eliminating the need for time-consuming computer simulations.

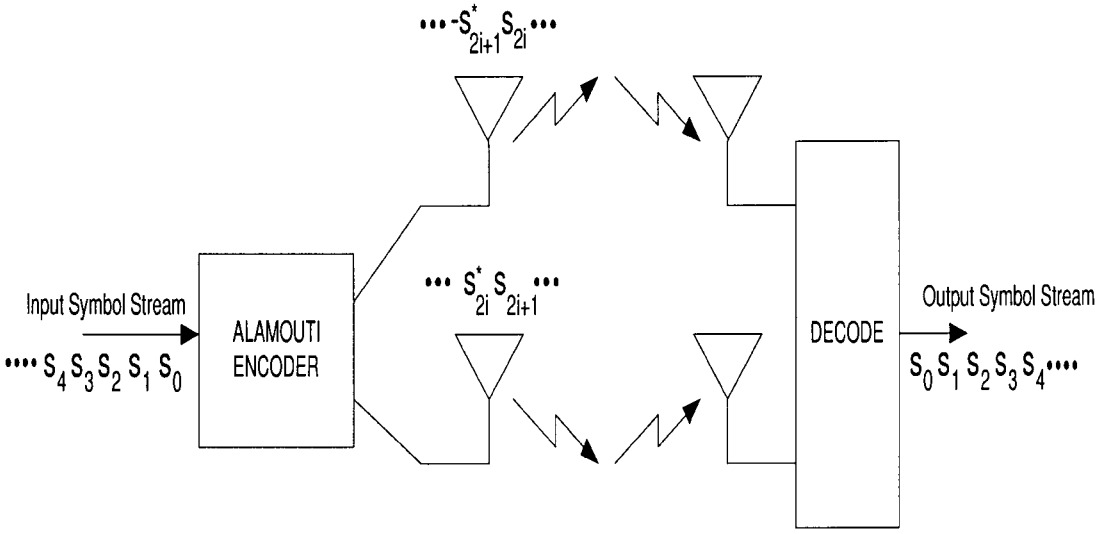

Figure 4. Alamouti scheme.

4.2. ALAMOUTI SCHEME

Transmit diversity schemes exploit spatial diversity inherent in MIMO systems to improve link reliability. In this paper, we consider the performance of a simple transmit diversity scheme, the Alamouti scheme [9], for the polarization diversity channel under consideration. A schematic of the transmission strategy for the Alamouti scheme is shown in Figure 4. Unlike the case of spatial multiplexing, in the Alamouti scheme redundancy is introduced in the transmitted symbol stream to exploit spatial diversity. More specifically, if symbols s_0 and s_1 are transmitted at polarizations +45° and –45° respectively during one symbol period, then during the following symbol period, symbols $-s_1^*$ and s_0^* are launched at polarizations +45° and –45°, respectively. We assume that the channel remains constant over at least two consecutive symbol periods and that the receiver has perfect channel knowledge and performs ML detection. The ML receiver for the Alamouti scheme is much simpler than that for spatial multiplexing. This is due to the fact that the structure of the transmitted signal orthogonalizes the channel irrespectively of the channel realization [9]. Appropriate processing at the receiver effectively turns the vector detection problem into simpler scalar detection problems. An estimate $\bar{P}_{div}$ of the average (over the random channel) uncoded symbol error rate for the Alamouti scheme as a function of the channel statistics was derived in [10]. We note that this estimate reveals all the trends of the actual symbol error rate and can predict performance of the Alamouti scheme accurately.

5. Measurement Results

Since the Alamouti scheme introduces redundancy in the transmitted data stream, the data rate will be half the data rate for spatial multiplexing if the same underlying scalar constellation is used. In order to compare the two signaling schemes at the same data rate, we employ a higher order constellation for the Alamouti scheme in our simulations. In particular, we assume that the data symbols for spatial multiplexing are drawn from a 4-QAM constellation while the data symbols for the Alamouti scheme are drawn from a 16-QAM constellation.

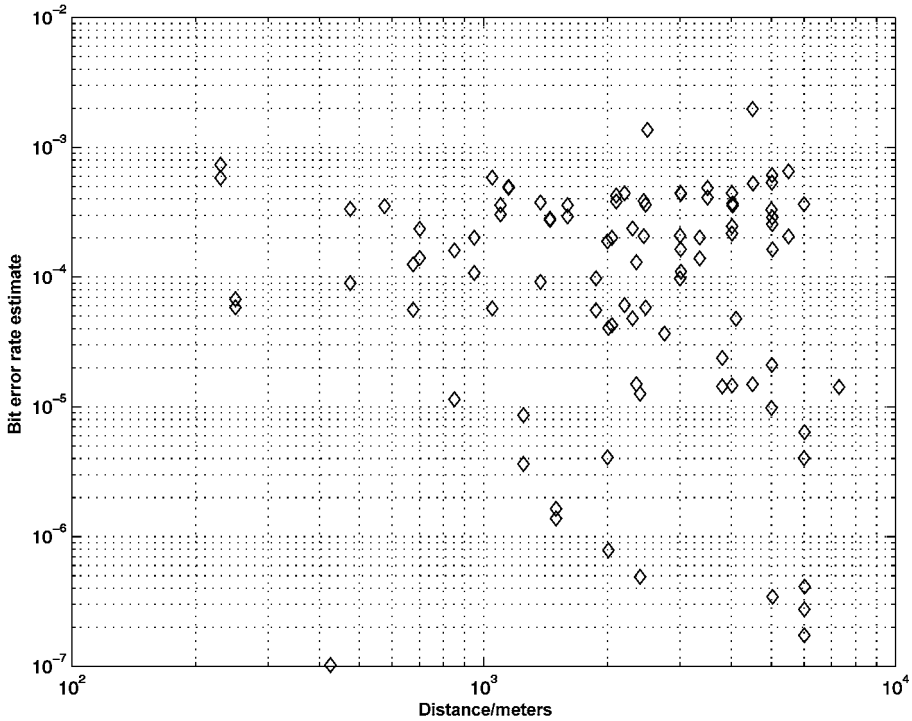

Figure 5. BER estimate for spatial multiplexing.

This ensures that data is transmitted at 4 bits/symbol period for both schemes. Additionally, we assume an SNR of 20 dB at each location. The assumption of fixed SNR is justified for systems employing power control. In order to compare the two schemes based on BER we make the following approximations $\mathrm{BER}_{mux} \approx \frac{\bar{P}_{mux}}{2}$ and $\mathrm{BER}_{div} \approx \frac{\bar{P}_{div}}{4}$, where BER_{mux} is the average bit error rate estimate for spatial multiplexing and BER_{div} is the average bit error rate estimate for the Alamouti scheme.

Figure 5 shows the BER estimate for spatial multiplexing as a function of distance from the base-station. It can be seen that BER_{mux} fluctuates widely over the cell, more so at greater distances from the base-station. The fluctuation can be attributed to the wide variation in channel statistics over the cell. Figure 6 shows the BER estimate for the Alamouti scheme as a function of distance from the base-station. As for the case of spatial multiplexing, BER_{div} fluctuates widely over the cell.

From Figures 5 and 6 it is clear that if knowledge of the channel statistics is available to the transmitter, the correct choice of transmission mode can result in significant BER improvements. For example, consider the measurement location closest to the base-station (at a distance of approximately 200 m). A comparison of the performance of the two schemes for this location reveals that the channel statistics at this point are much more conducive to the Alamouti scheme than they are for spatial multiplexing. If feedback were available, the choice of the Alamouti scheme over spatial multiplexing would result in nearly two orders of magnitude reduction in BER. In Figure 7, we plot $\frac{\max(\mathrm{BER}_{mux},\mathrm{BER}_{div})}{\min(\mathrm{BER}_{mux},\mathrm{BER}_{div})}$ for each measurement location. The plot reveals the reduction in BER possible through correct selection of the transmission mode for each measurement location and clearly illustrates the value of feedback of channel statistics to the transmitter for mode selection. Feeding pertinent channel statistics back to the

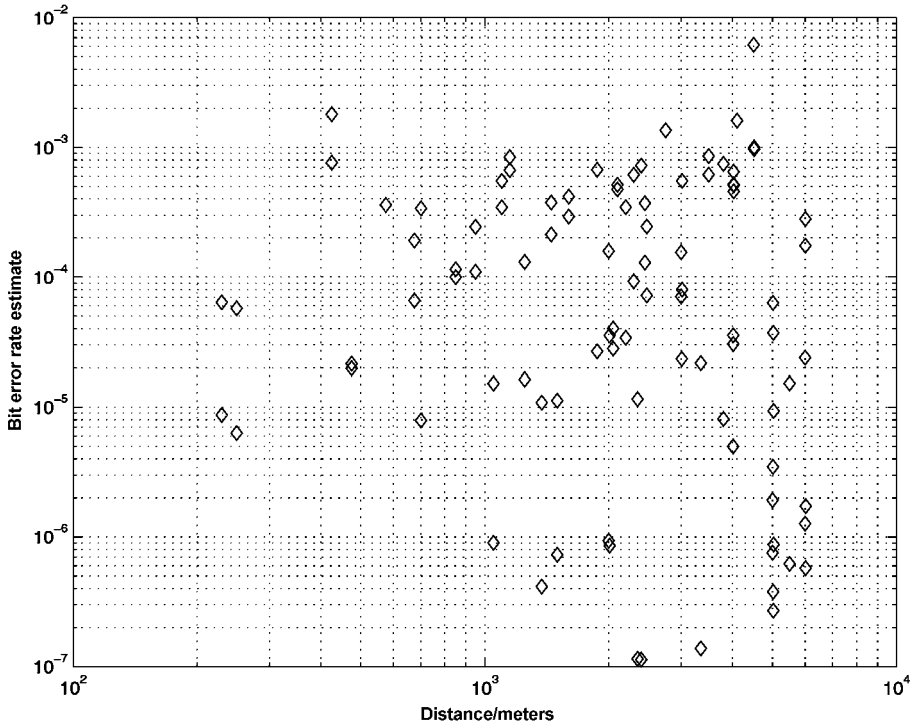

Figure 6. BER estimate for the Alamouti scheme.

transmitter can be accomplished via a low-bandwidth link. Furthermore, conveying channel statistics to the transmitter is more easily accomplished than feeding back the channel state information itself.

If feedback is not available, it is beneficial to note the general trend in performance of spatial multiplexing and the Alamouti scheme over the cell area. In Figure 8, we plot the least-squares line fit for both spatial multiplexing and the Alamouti scheme data points. The plot reveals the existence of a switching point at about 1 km from the base-station. We refer to this distance as the preferred-mode switching distance – one mode of transmission is typically preferred over the other, depending on the subscriber's position relative to the switching distance. We stress that choice of the transmission strategy based solely on the subscriber's position relative to the preferred-mode switching distance may not be optimal. However, in the absence of feedback, the preferred-mode switching distance is a fair indicator of the preferred-mode of transmission. For the cell under consideration, spatial multiplexing is the preferred transmission strategy for locations that are less than 1 km away from the base-station, while the Alamouti scheme is preferred for locations closer to the cell edge. This can be attributed to the fact that the MIMO channel experienced by users closer to the base-station tends to have higher rank due to large angle spreads, which favors spatial multiplexing. Users at the edge of the cell tend to experience smaller angle spreads and hence increased spatial fading correlation which is detrimental to spatial multiplexing.

The preferred-mode switching distance for a cell will be a function of the SNR, data rate, and the channel statistics inherent to the cell topology. Moreover, the use of forward error correction coding can be expected to have a significant impact on the preferred-mode switching distance as well. The results in this paper assume equal SNR at all locations within

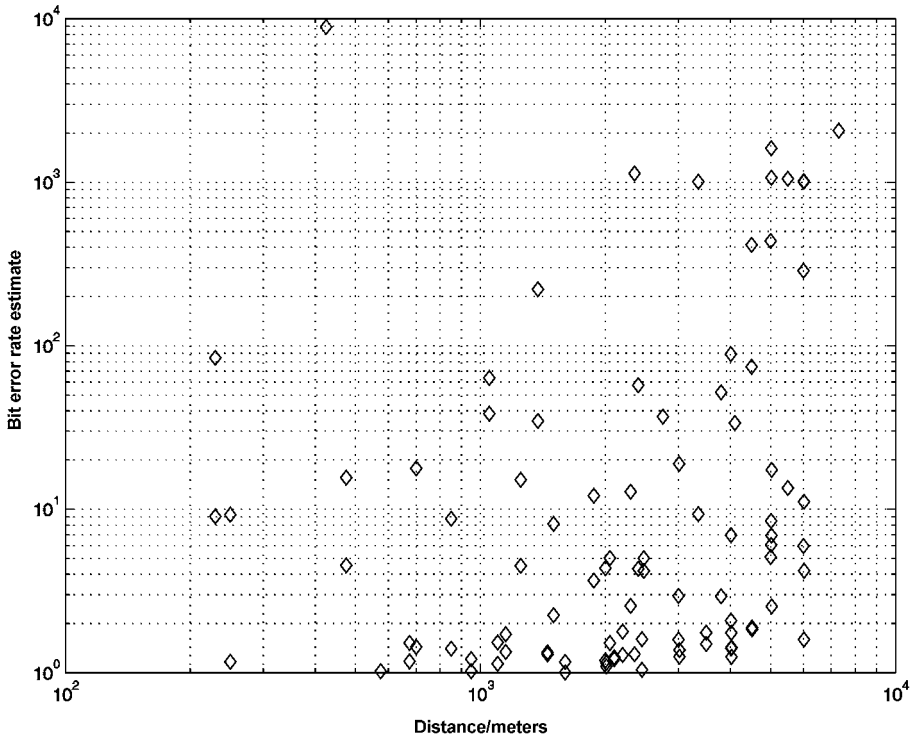

Figure 7. Reduction in BER through optimal mode selection.

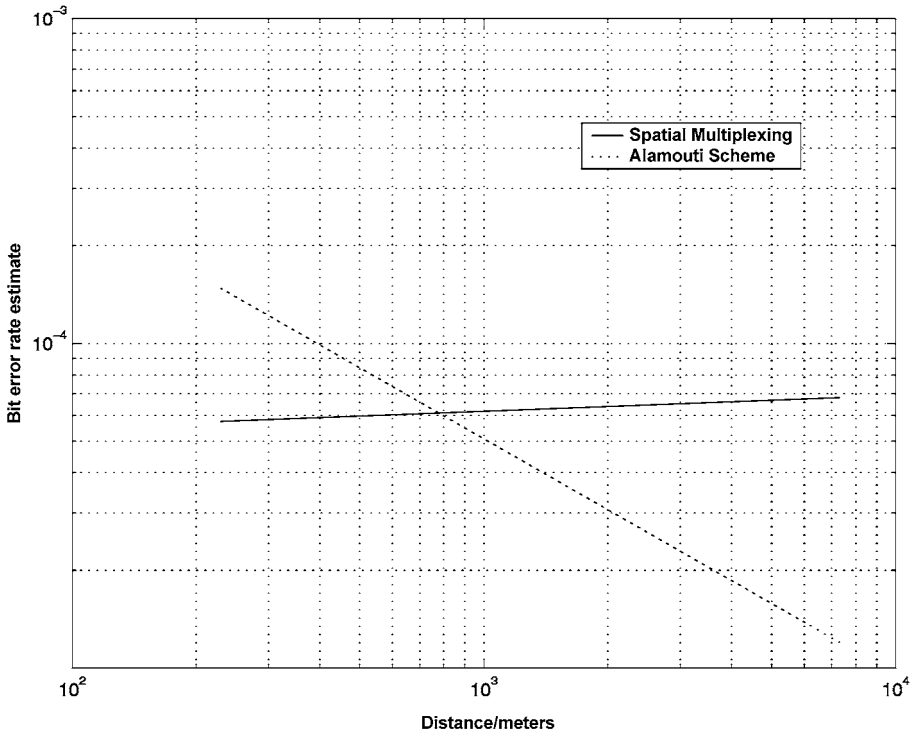

Figure 8. Preferred-mode switching distance.

the cell. Alternatively, we can set the SNR at each location to be a function of the distance from the base-station and the path-loss exponent measured for the cell. Similar performance trend lines can be plotted for the two schemes for this scenario and a preferred-mode switching distance can be established.

6. Conclusions

We studied the performance of spatial multiplexing and the Alamouti scheme in terms of average bit error rate for a dual-polarized antenna system using data acquired through channel measurements. The results motivate the use of feedback of channel statistics to the transmitter for link adaptation. Appropriate choice of the transmission mode based on channel statistics information can improve the bit error rate by several orders of magnitude. Furthermore, the existence of a preferred-mode switching distance within the cell was established. For the cell under consideration, the channel statistics are more conducive to spatial multiplexing closer to the base-station, while the Alamouti scheme is preferred for locations closer to the cell edge.

Acknowledgments

R.U. Nabar's work was supported by the Dr. T.J. Rodgers Stanford Graduate Fellowship. The work of H. Bölcskei was supported by FWF grant J1868-TEC and by NSF grants CCR 99-79381 and ITR 00-85929. The authors would like to thank D. Baum and S. Pitchaiah of Iospan Wireless Inc., San Jose, CA and D. Gore of Stanford University for their invaluable contributions to the measurement campaign.

References

1. A.J. Paulraj and T. Kailath, "Increasing Capacity in Wireless Broadcast Systems Using Distributed Transmission/Directional Reception", U.S. Patent, No. 5,345,599, 1994.
2. I.E. Telatar, "Capacity of Multi-Antenna Gaussian Channels", *European Trans. Tel.*, Vol. 10, No. 6, pp. 585–595, 1999.
3. G.J. Foschini, "Layered Space-Time Architecture for Wireless Communication in a Fading Environment When Using Multi-Element Antennas", *Bell Labs Tech. J.*, pp. 41–59, 1996.
4. G.J. Foschini and M.J. Gans, "On Limits of Wireless Communications in a Fading Environment When Using Multiple Antennas", *Wireless Personal Communications*, Vol. 6, pp. 311–335, 1998.
5. H. Bölcskei, D. Gesbert and A.J. Paulraj, "On the Capacity of OFDM-Based Spatial Multiplexing Systems", *IEEE Trans. Comm.*, Vol. 50, No. 2, pp. 225–234, 2002.
6. J. Guey, M. Fitz, M. Bell and W. Kuo, "Signal Design for Transmitter Diversity Wireless Communication Systems over Rayleigh Fading Channels", in *Proc. IEEE VTC*, Atlanta, GA, April/May 1996, Vol. 1, pp. 136–140.
7. V. Tarokh, N. Seshadri and A.R. Calderbank, "Space-Time Codes for High Data Rate Wireless Communication: Performance Criterion and Code Construction", *IEEE Trans. Inf. Theory*, Vol. 44, No. 2, pp. 744–765, 1998.
8. V. Tarokh, H. Jafarkhani and A.R. Calderbank, "Space-Time Block Codes from Orthogonal Designs", *IEEE Trans. Inf. Theory*, Vol. 45, No. 5, pp. 1456–1467, 1999.
9. S.M. Alamouti, "A Simple Transmit Diversity Technique for Wireless Communications", *IEEE J. Sel. Areas Comm.*, Vol. 16, No. 8, pp. 1451–1458, 1998.
10. R.U. Nabar, H. Bölcskei, V. Erceg, D. Gesbert and A.J. Paulraj, "Performance of Multi-Antenna Signaling Techniques in the Presence of Polarization Diversity", *IEEE Trans. Sig. Proc.*, Vol. 50, No. 10, Oct. 2002.

11. H. Bölcskei, R.U. Nabar, V. Erceg, D. Gesbert and A.J. Paulraj, "Performance of Spatial Multiplexing in the Presence of Polarization Diversity", in *Proc. IEEE ICASSP*, Salt Lake City, UT, May 2001, Vol. 4, pp. 2437–2440.
12. R. Heath and A.J. Paulraj, "Switching between Multiplexing and Diversity Based on Constellation Distance", in *Proc. Allerton Conf. on Comm. Control and Comp.*, Monticello, Illinois, Sept./Oct. 2000.
13. D.S. Baum, D.A. Gore, R.U. Nabar, S. Panchanathan, K.V.S. Hari, V. Erceg and A.J. Paulraj, "Measurement and Characterization of Broadband MIMO Fixed Wireless Channels at 2.5 GHz", in *Proc. IEEE Int. Conf. on Personal Wireless Comm.*, Hyderabad, India, Dec. 2000, pp. 203–206.
14. G.L. Stüber, *Principles of Mobile Communication*, Kluwer Academic Publishers, Norwell, MA, 1996.

Rohit U. Nabar was born in Bombay, India on Dec. 18, 1976. He received the B.S. (*summa cum laude*) degree in electrical engineering from Cornell University, Ithaca, NY in 1998 and the M.S. degree in electrical engineering from Stanford University, Stanford, CA in 2000. He successfully defended his Ph.D. thesis at Stanford University in August 2002 where he was also the recipient of the Dr. T.J. Rodgers Stanford Graduate Fellowship. He is currently a postdoctoral researcher at the Communication Technology Laboratory ETH Zürich. His research interests are in the areas of signal processing for wireless communications and multi-input multi-output (MIMO) antenna systems.

Vinko Erceg received the B.S.E.E. in 1988 and the Ph.D.E.E. in 1992, both from the City University of New York. From 1990 to 1992, he was a lecturer at the Electrical Engineering Department at the City College of NY, concurrently working with SCS Mobilecom, Port

Washington, NY, on spread-spectrum systems for mobile communications. In 1992, he joined AT& T Bell Laboratories and became a principal member of technical staff in the Wireless Communications Research Department of AT& T Labs-Research in 1996. He participated in various aspects of wireless research, including signal propagation modeling, communication systems engineering and performance analysis. From February 2000 to August 2002, he was with Iospan Wireless, San Jose, CA where he served as Director and Principal Engineer of channel modeling and systems validation. Since September 2002 he has been with Zyray Wireless, San Diego, CA. His research interests include radio propagation, capacity, performance, and coverage prediction of cellular and MIMO wireless systems. Dr. Erceg chaired the IEEE 802.16 working group on broadband wireless access standards in developing NLOS channel models in 2001.

Helmut Bölcskei was born in Mödling, Austria on May 29, 1970. He received the Dipl.-Ing. and Dr. Techn. degrees in electrical engineering/communications from Vienna University of Technology, Vienna, Austria, in 1994 and 1997, respectively. From 1994 to 2001 he was with the Institute of Communications and Radio-Frequency Engineering, Vienna University of Technology. From March 2001 to January 2002, he was an assistant professor of electrical engineering at the University of Illinois at Urbana-Champaign. Since February 2002 he has been an assistant professor of communication theory at ETH Zurich. He was a visiting researcher at Philips Research Laboratories Eindhoven, The Netherlands, ENST Paris, France, and the Heinrich-Hertz-Institute Berlin, Germany. From February 1999 to February 2001 he was a postdoctoral researcher in the Smart Antennas Research Group in the Information Systems Laboratory, Department of Electrical Engineering, Stanford University, Stanford, CA. From 1999–2001 he was a consultant for Iospan Wireless Inc. (formerly Gigabit Wireless Inc.). His research interests include communication and information theory and statistical signal processing with special emphasis on wireless communications, multi-input multi-output (MIMO) antenna systems, space-time coding, Orthogonal Frequency Division Multiplexing (OFDM), and wireless networking. He received a 2001 IEEE Signal Processing Society Young Author Best Paper Award and was an Erwin Schrödinger Fellow (1999–2001) of the Austrian National Science Foundation (FWF). He serves as an associate editor for the IEEE Transactions on Wireless Communications and the IEEE Transactions on Signal Processing.

Arogyaswami J. Paulraj has been a professor at the Department of Electrical Engineering, Stanford University since 1993, where he supervises the Smart Antennas Research Group. This group consists of approximately a dozen researchers working on applications of space-time signal processing for wireless communications networks. His research group has developed many key fundamentals of this new field and helped shape a worldwide research and development focus on this technology. Paulraj was educated at the Naval Engineering College and the Indian Institute of Technology, Delhi, India (Ph.D. 1973). His non-academic positions included Head, Sonar Division, Naval Oceanographic Laboratory, Cochin; Director, Center for Artificial Intelligence and Robotics, Bangalore; Director, Center for Development of Advanced Computing; Chief Scientist, Bharat Electronics, Bangalore, and Chief Technical Officer and Founder, Iospan Wireless Inc. He has also held visiting appointments at the Indian Institute of Technology, Delhi, Loughborough University of Technology, and Stanford University. Paulraj sits on several boards of directors and advisory boards for U.S. and Indian companies/venture partnerships. Paulraj's research has spanned several disciplines, emphasizing estimation theory, sensor signal processing, parallel computer architectures/algorithms and space-time wireless communications. His engineering experience includes development of sonar systems, massively parallel computers, and more recently broadband wireless systems. Paulraj has won several awards for his engineering and research contributions. These include two President of India Medals, CNS Medal, Jain Medal, Dist. Service Medal, Most Dist. Service Medal, VASVIK Medal, IEEE Best Paper Award (Joint), amongst others. He is the author of over 250 research papers and holds eight patents. Paulraj is a fellow of the Institute of Electrical and Electronics Engineers (IEEE) and a member of the Indian National Academy of Engineering.